



432 4

A Fluid Mechanics Model to Estimate the Leakage of Incompressible Fluids Through Labyrinth Seals

J. T. Han

Any information contained herein is unclassified unless otherwise indicated. This report was prepared for the U.S. Government under contract number W-31-109-ENG-54. It is the property of the U.S. Government and is loaned to your organization; it and its contents are not to be distributed outside your organization. This report is available to the public through the National Technical Information Service, Department of Energy.

OAK RIDGE NATIONAL LABORATORY

CENTRAL RESEARCH LIBRARY

CIRCULATION SECTION

4500N ROOM 175

LIBRARY LOAN COPY

DO NOT TRANSFER TO ANOTHER PERSON

If you wish someone else to see this report, send in name with report and the library will arrange a loan.

• • • • •

OAK RIDGE NATIONAL LABORATORY
OPERATED BY UNION CARBIDE CORPORATION • FOR THE DEPARTMENT OF ENERGY

Printed in the United States of America. Available from
the Department of Energy,
Technical Information Center
P.O. Box 62, Oak Ridge, Tennessee 37830
Price: Printed Copy \$4.50; Microfiche \$3.00

This report was prepared as an account of work sponsored by an agency of the United States Government. Neither the United States Government nor any agency thereof, nor any of their employees, contractors, subcontractors, or their employees, makes any warranty, express or implied, nor assumes any legal liability or responsibility for any third party's use or the results of such use of any information, apparatus, product or process disclosed in this report, nor represents that its use by such third party would not infringe privately owned rights.

ORNL/TM-6373
Dist. Category UC-79,
-79e, -79p

Contract No. W-7405-eng-26

Engineering Technology Division

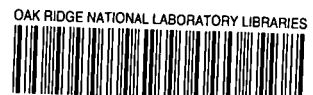
A FLUID MECHANICS MODEL TO ESTIMATE THE LEAKAGE OF
INCOMPRESSIBLE FLUIDS THROUGH LABYRINTH SEALS

J. T. Han

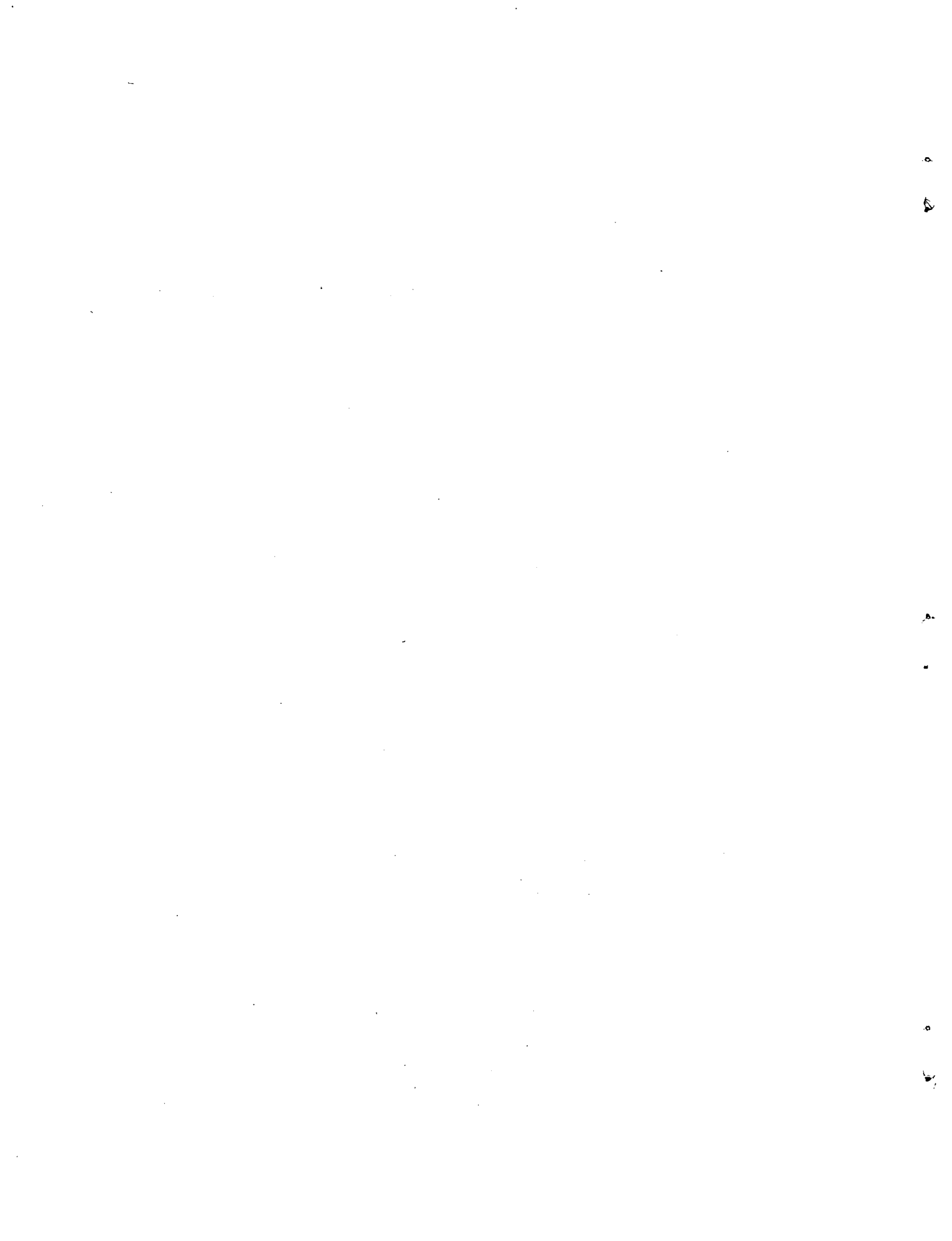
Date Published - August 1978

NOTICE: This document contains information of a preliminary nature. It is subject to revision or correction and therefore does not represent a final report.

Prepared by the
OAK RIDGE NATIONAL LABORATORY
Oak Ridge, Tennessee 37830
operated by
UNION CARBIDE CORPORATION
for the
DEPARTMENT OF ENERGY

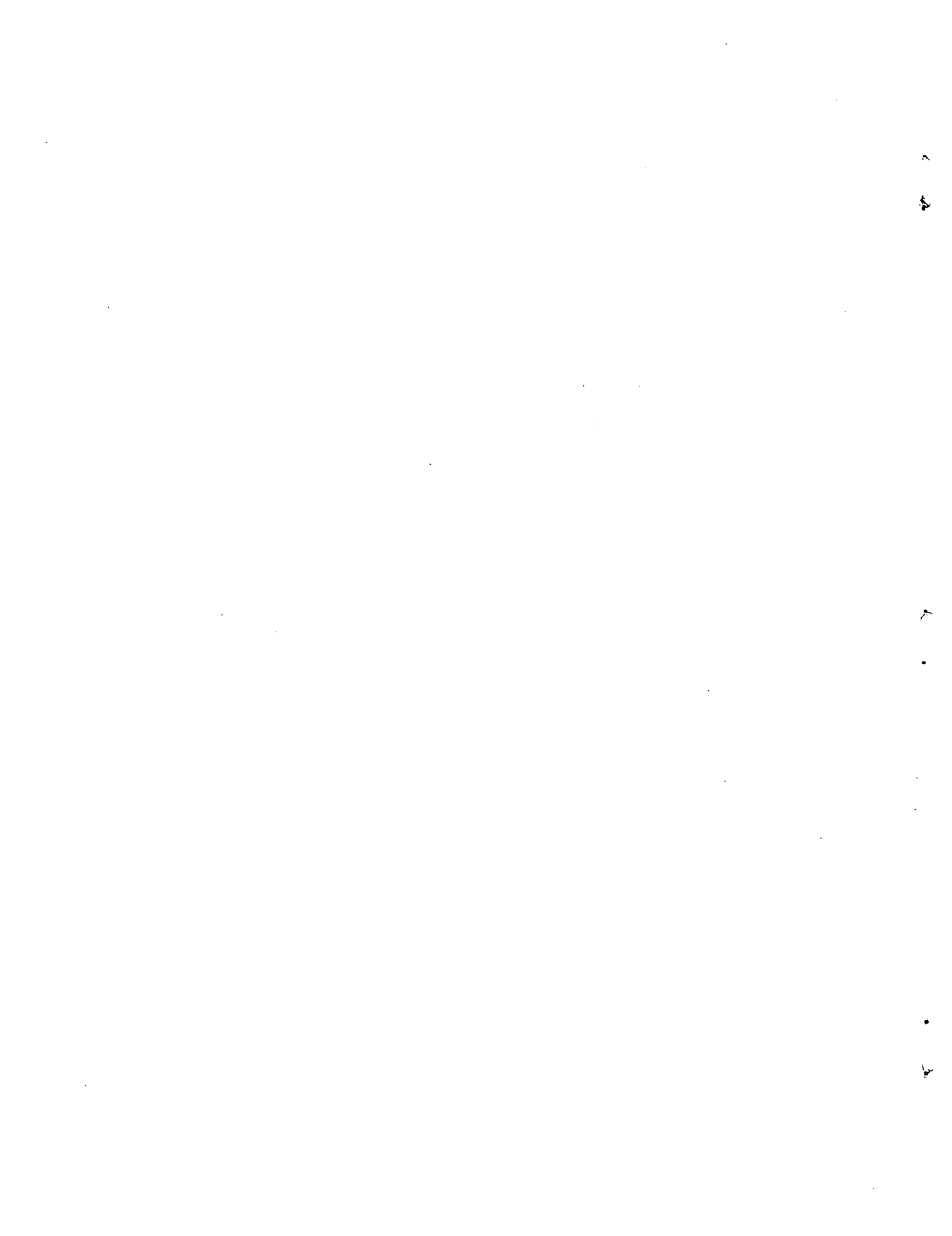


3 4456 0551432 4



CONTENTS

	<u>Page</u>
ABSTRACT	1
INTRODUCTION	1
ANALYTICAL MODEL	2
Labyrinth Seals with Rectangular Cavities	10
Labyrinth Seals with Helical Threads	11
RESULTS AND DISCUSSION	16
CONCLUSIONS	21
NOMENCLATURE	21
REFERENCES	23



A FLUID MECHANICS MODEL TO ESTIMATE THE LEAKAGE OF
INCOMPRESSIBLE FLUIDS THROUGH LABYRINTH SEALS

J. T. Han

ABSTRACT

An analytical model for estimating the leakage of incompressible fluids through straight labyrinth seals is described. Results from the model are in reasonable agreement with the limited data available. The mass leak rate is shown to be proportional to the seal clearance and pressure drop in the following functional dependency: $M \propto C^a (\Delta P)^b$, where $1.5 < a < 3$ and $0.5 < b < 1$.

INTRODUCTION

Labyrinth seals [1-7] have been used in steam turbines and compressors to reduce flow leakage for many years. These seals utilize a labyrinth path to increase resistance to flow.

Egli [1] developed a theoretical model for calculating the leakage of compressible fluids (gases). Using the ideal gas law and assuming isentropic expansion for the gas passing through each throttling passage of the seal, he derived an equation showing leakage as a function of seal inlet pressure and specific volume, seal outlet pressure, and total number of throttlings in the seal. However, empirical coefficients in his equation were determined from superheated steam data. Other similar analytical studies and empirical correlations for gases can also be found in the literature [2-7].

Recently, labyrinth seals have been used in the test section of two sodium-cooled THORS pin bundles [8,9] to reduce the leakage and to account for the differential thermal expansion between the heated test section and its housing. The correlations for gases [1-7] are probably inapplicable to sodium, and therefore a method for estimating the leakage of incompressible fluids through labyrinth seals was needed.

This report presents an analytical model for estimating the leakage of incompressible fluids through straight labyrinth seals. Recent developments [10-28] in theoretical (including numerical solutions) and

experimental studies of the recirculating flow inside rectangular cavities and of the channel flow between parallel plates (including the entrance and exit effects) have been incorporated into the model. The approach used in the model is different from that of previous ones in which the gas-dynamics laws with some empirically determined coefficients were used.

In the present model, as well as previous ones [1-7], the straight labyrinth seal is assumed to be stationary. The effect caused by the rotating shaft of some of the seals has been experimentally found to be small [1]. Furthermore, the analytical results by Tao and Donovan [29] have also indicated that the rotating effect of the shaft is insignificant for flow in a narrow annulus.

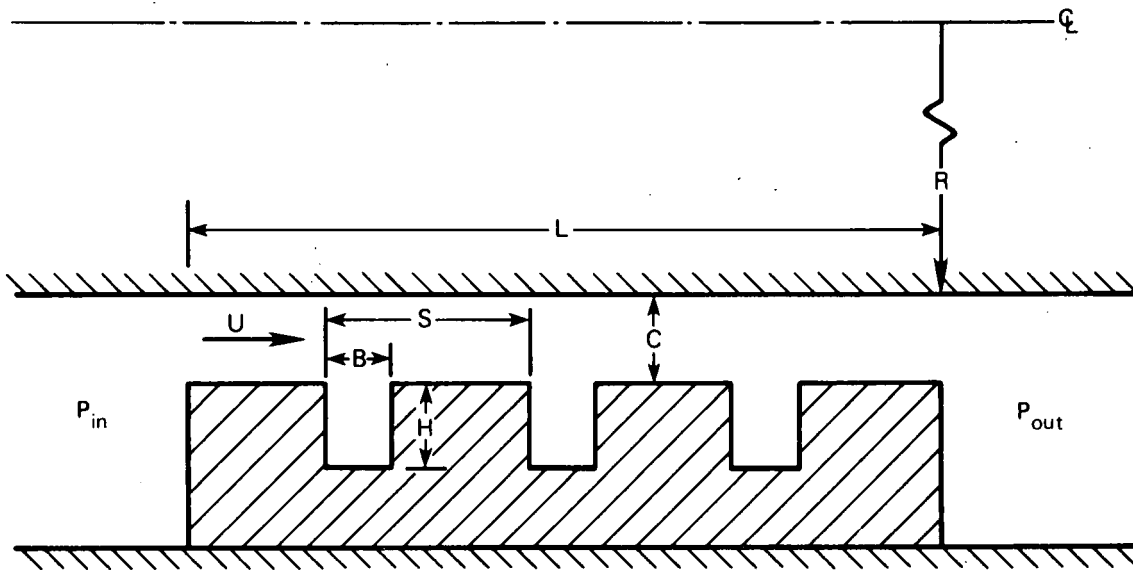
ANALYTICAL MODEL

Labyrinth seals are normally used in annular passages. Figure 1 shows the two kinds of straight labyrinth seals discussed here: rectangular cavity and helical thread types. Assumptions used in the present model are (1) constant fluid properties based on average temperature and pressure in the seal; (2) $R/C \gg 1$ for cavity-type seals (see Nomenclature for definition of symbols) and $R/C \gg 1$ and also $2\pi R/S \gg 1$ for helical-thread-type seals so that the flow can be treated as two dimensional in the seal; (3) finite cavities and threads (e.g., $H/B \leq 5$ and $A/B \leq 5$); and (4) $Re_c = UB/\nu \geq$ an order of 100.

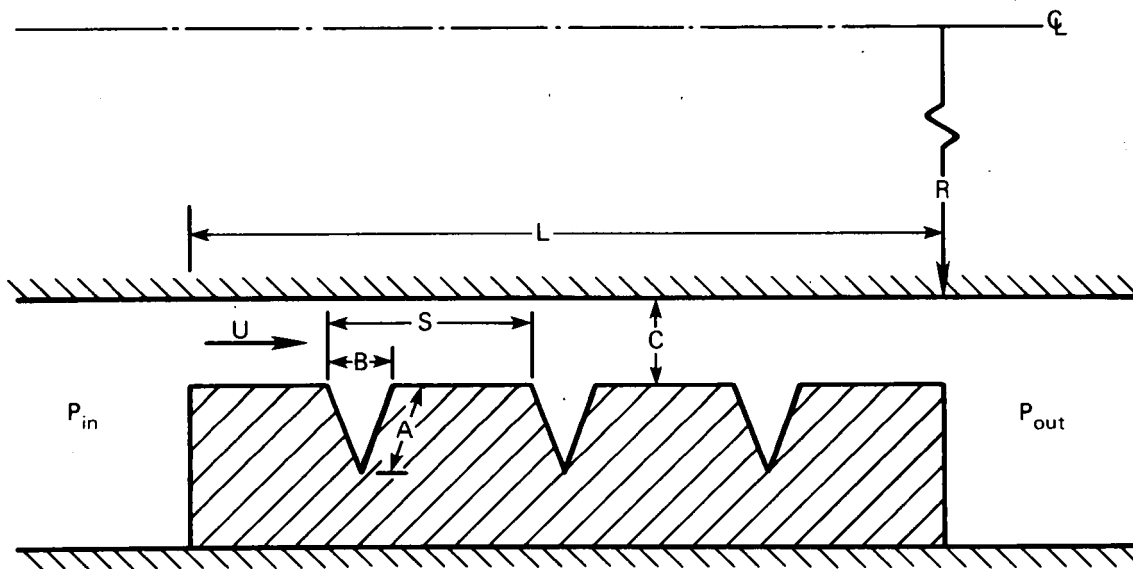
The flow of fluid through the seal is driven by the pressure difference between the seal inlet and outlet. Letting ΔP be the "average" driving pressure drop across each throttling of the seal (as represented in Fig. 2),

$$\Delta P = \frac{1}{N} \left[P_{in} - P_{out} - C_1 \rho g L - (K_c + K_e) \frac{\rho U^2}{2} \right], \quad (1)$$

where $C_1 = 0$ if the seal inlet and outlet are at the same elevation and $C_1 = 1$ (or $C_1 = -1$) if the seal inlet is located vertically below (or above) the outlet. The last term in Eq. (1) is the pressure loss caused by the contraction and expansion of flow area at the seal inlet and outlet, respectively [10].



(a)



(b)

Fig. 1. Two kinds of straight labyrinth seals: (a) rectangular cavity, (b) helical thread.

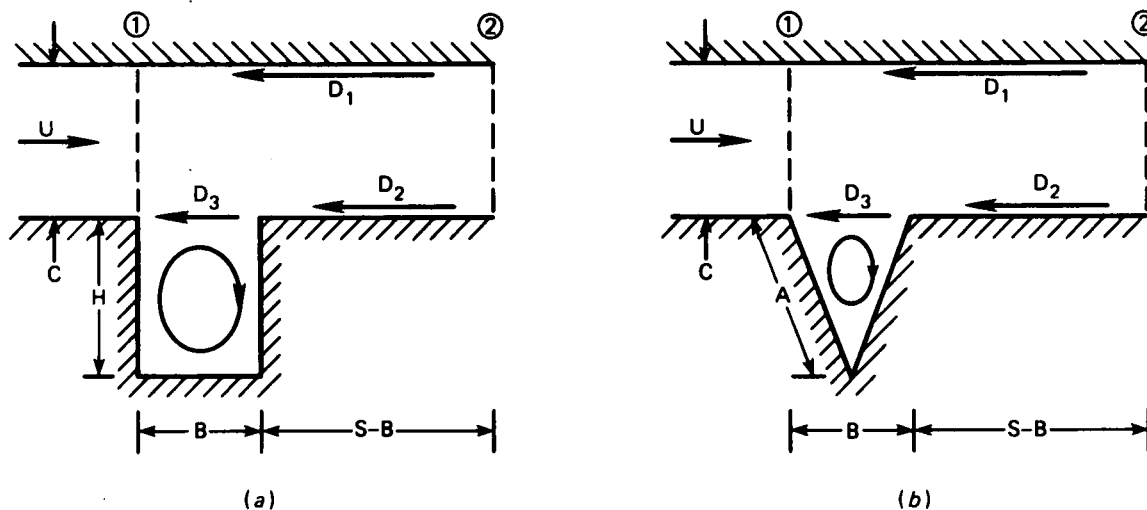


Fig. 2. Friction drags in a unit of seal throttling: (a) rectangular cavity, (b) helical thread.

For fully developed flow in the channel between two parallel plates [11], ΔP is equal to the sum of various friction drags exerted on the flow by the inner wall (D_1), the outer wall (D_2), and the cavity flow (D_3) as shown in Fig. 2. Thus,

$$\Delta P = (D_1 + D_2 + D_3)/(CW) . \quad (2)$$

For flow in the hydrodynamic entry length of the channel [11], the right-hand side of Eq. (2) should include a term to account for the increase in the total fluid momentum flux between the outlet and inlet of the throttling. To simplify the equation, the momentum flux term is included in the terms of D_1 and D_2 to be defined later. There is no gravity term in Eq. (2) because it has already been taken into account in Eq. (1).

The incompressible flow in the channel is approximated by the ideal channel flow without the presence of cavities or threads and can be either laminar or turbulent, depending on its Reynolds number. For laminar flow in the channel [11] with $Re = U2C/\nu \leq 2000$, we have

$$D_1 = 6C_2\rho\nu SWU/C \quad (3)$$

and

$$D_2 = 6C_2\rho\nu(S - B)WU/C , \quad (4)$$

where C_2 is the laminar entry-length coefficient to account for the larger pressure drop in the hydrodynamic entry length (above that in the fully developed region) caused by the increase in the fluid momentum flux and a larger viscous friction at the wall. (C_2 is generally greater than unity and will be approximately equal to unity for the channel flow with a much longer, fully developed region than the hydrodynamic entry length.)

For turbulent flow in the channel with $Re > \sim 2000$, friction drags are given either in empirical formulas or in the Moody diagram [12]. The Blasius formula was chosen for the present study because of its simplicity and accuracy:

$$\tau_0 = 0.03955 \rho U^2 Re^{-0.25} , \quad (5)$$

which is in excellent agreement with experimental data, at least up to $Re = 100,000$.

Substituting Eq. (5) into $D_1 = C_3\tau_0SW$ and $D_2 = C_3\tau_0(S - B)W$ yields

$$D_1 = 0.0333C_3\rho(\nu/C)^{0.25} SWU^{1.75} \quad (6)$$

and

$$D_2 = 0.0333C_3\rho(\nu/C)^{0.25} (S - B)WU^{1.75} , \quad (7)$$

where C_3 is the turbulent entry-length coefficient ($C_3 \geq 1$).

The magnitude of drag D_3 is equal to the shear force of the channel flow exerted on the cavity flow (or flow inside the thread) to maintain it in motion; therefore, D_3 is equal to the flow resistance exerted on the cavity flow by the cavity walls (two side walls and one bottom wall). In order to estimate the value of D_3 , one must understand the characteristics of the flow inside the cavity (or thread).

A number of experimental and theoretical (including numerical solutions of the governing equations) studies have been performed to investigate the recirculating flow inside rectangular cavities of various height-to-breadth ratios [13-28]. Batchelor [13] proposed that at large Reynolds

numbers ($Re_c = UB/\nu$), two-dimensional cavity flow can be divided into two regions: an inviscid core of uniform vorticity and a boundary-layer region adjacent to the wall, as shown in Fig. 3. Based on Batchelor's idea, Squire [14,15] solved the laminar boundary layer equation for flow inside a cylinder. Roshko [15,16] obtained velocity and pressure profiles on the walls of a square cavity ($H = B = 102$ mm) in a wind tunnel. Figure 4 shows his velocity measurements along the line normal to the midpoint on each of the cavity walls at two external velocities; it is clearly shown that the boundary-layer region does exist along the cavity walls, as Batchelor suggested. Furthermore, the velocity at the outer edge of the boundary layer (U_c) is approximately 25 to 45% of the external velocity.

Although the boundary layer on the cavity walls (Fig. 4) will be somewhat different from that on a flat plate because of pressure variations [16] inside the cavity, it is assumed in the present study that the boundary layer along each of the three cavity walls is approximated by that on a flat plate. (For instance, the boundary layer along the bottom wall is approximated by that on a flat plate with its origin at the lower right corner of the cavity.) If we introduce a modified cavity Reynolds number (Re_ρ) based on the maximum boundary layer velocity (taken $U_c = 0.4U$) instead of external velocity (U), its value (using air properties at

ORNL DWG 78 4769

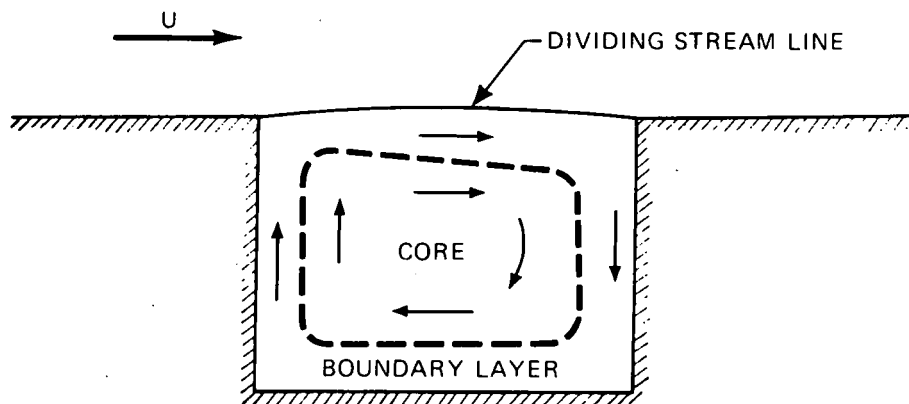


Fig. 3. Batchelor's cavity-flow model: an inviscid core of uniform vorticity surrounded by a boundary layer region (Squire [14]).

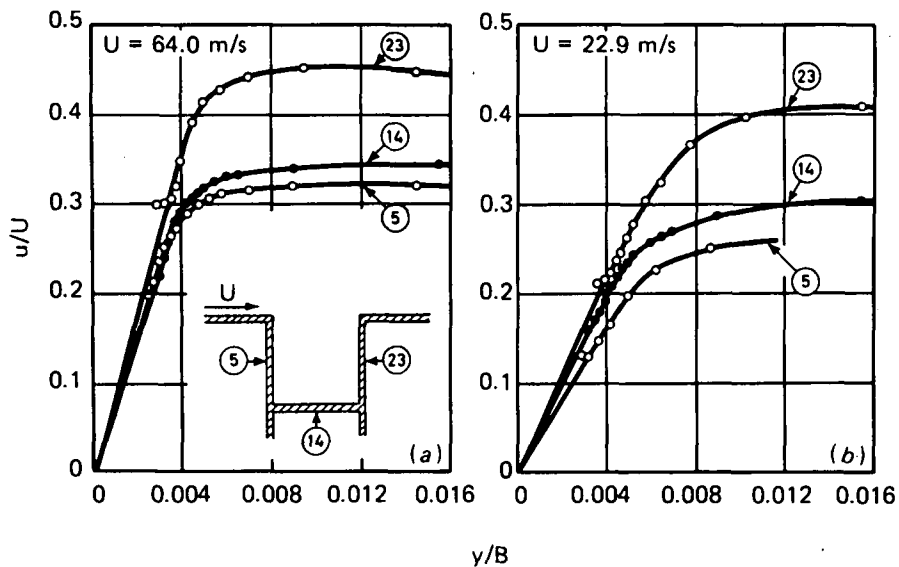


Fig. 4. Experimental velocity profiles on the walls of a square cavity ($H = B = 102$ mm) at two external velocities (Roshko [16]).

room temperature) is found to be 170,000 and 61,000, respectively, corresponding to $U = 64.0$ and 22.9 m/s (Fig. 4). These values are still below the upper limit of the Reynolds number, approximately at 500,000 for the laminar boundary layer on a flat plate [12]. Using Blasius' solution [12] with $\delta = 5.0 [\nu B / (2U_c)]^{0.5}$, one finds the laminar boundary-layer thickness at the midpoint of each of three cavity walls (note that $H = B$) to be at $\delta/B = 0.0086$ and 0.014 , respectively, for $U = 64.0$ and 22.9 m/s. These values are in excellent agreement with Roshko's experiment (Fig. 4). Therefore, the use of flat-plate boundary-layer approximation is justified, at least for Roshko's experiment.

Batchelor [13] did not specify the lower limit of the cavity Reynolds number (Re_c) to sustain the boundary-layer flow on the cavity walls. However, from Roshko's experiment (Fig. 4) at cavity Reynolds numbers of the order of 100,000, the boundary-layer flow did exist. All other experimental investigations [17-21] were devoted to flow visualization studies to determine the sizes and locations of recirculating vortices inside rectangular cavities of various height-to-breadth ratios; and therefore, it cannot

be determined from those studies whether or not the boundary layer flow exists along the cavity wall.

Numerical studies for laminar cavity flow have been reported in the literature [17-18, 22-28]. Either the full Navier-Stokes equations or the creep flow equations ($Re_c \rightarrow 0$) were solved numerically on a computer with Re_c as high as 50,000. Figure 5 shows the streamlines and vorticity distributions inside a square cavity calculated by Burggraf [22] (with the top wall moving from the right to left). At $Re_c \leq 100$, there is no such core region of constant vorticity; however, at $Re_c = 400$, the central region of the cavity has a somewhat uniform vorticity. Figure 6 shows Burggraf's velocity profiles on the vertical centerline of the square cavity at various values of Re_c . (He obtained the result analytically at $Re_c \rightarrow \infty$ by using a linearized model for an eddy bounded by a circular streamline.) If the Blasius solution [12] is used to estimate the boundary-layer thickness at the midplane of the bottom wall with $Re_c = 400$ (arbitrarily using air properties at room temperature, $U_c = 0.3U$ as shown in Fig. 6, $U = 0.4$ m/s, and B calculated from $Re_c = 400$ as 0.015 m), a value of $\delta = 0.32B$ is obtained; this value is in excellent agreement with that shown in Fig. 6 with the peak velocity at $\delta/B = Y/B = 0.3$. Therefore, in this report it is assumed that the boundary-layer flow exists along the cavity walls at Re_c of approximately 400 or higher. Note that the corresponding boundary-layer Reynolds number in the cavity ($Re_\delta = U_c B/\nu = C_4 Re_c$, where $0.25 \leq C_4 \leq 0.62$ as shown in Figs. 4 and 6) is at least 100 or higher, which indeed satisfies the Prandtl assumption [12] that the Reynolds number should be at least two orders of magnitude greater than unity in order to have boundary-layer flow on a wall. (It is worth noting that in a recent paper, Nallasamy and Krishna Prasad [23] concluded from their numerical solutions for square-cavity flow that only at $Re_c \geq 30,000$ will the cavity flow "completely" correspond to the Batchelor model, where an inviscid core of uniform vorticity is surrounded by a boundary-layer region next to the wall. However, the author believes that the value of 30,000 is much too high for practical applications because the calculated vorticity variations in the entire cavity core at $Re_c = 30,000$ are very small - less than 1% from a constant value as shown in [23].)

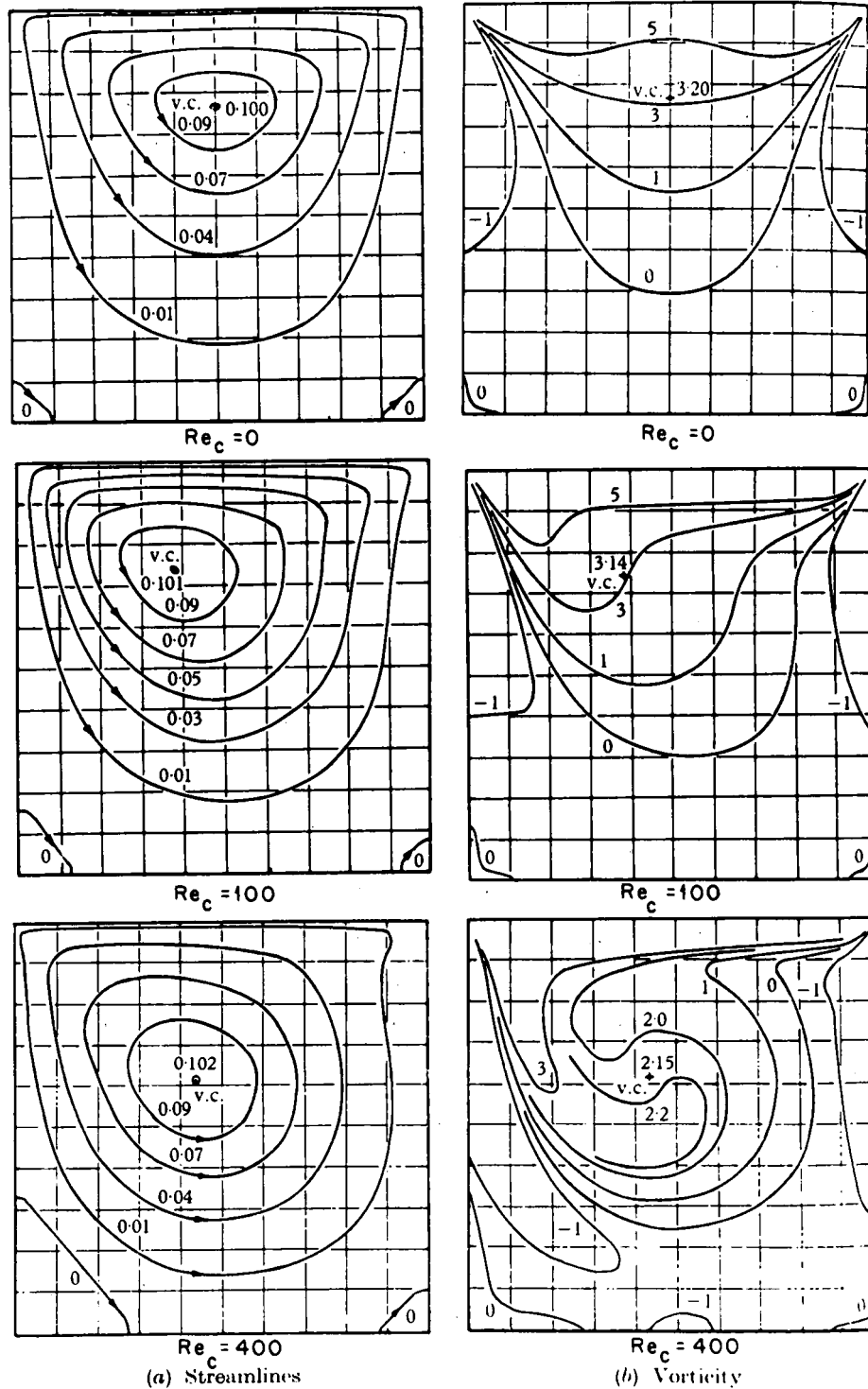


Fig. 5. Streamlines and vorticity distributions inside a square cavity. Note that the dimensionless values of the stream function and vorticity are shown respectively in (a) and (b) (Burggraf [22]).

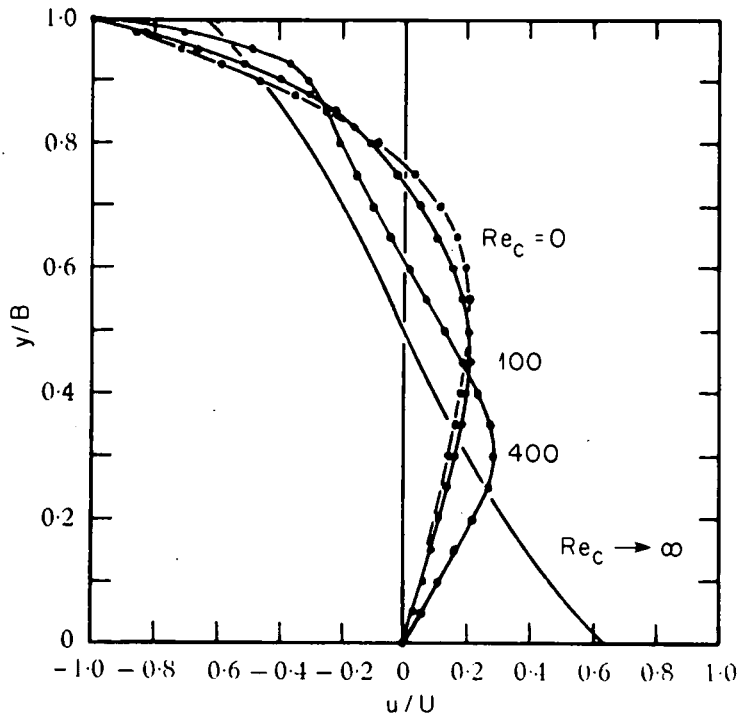


Fig. 6. Velocity profiles on vertical centerline of a square cavity (Burggraf [22]).

In summary, in the present model the boundary-layer region on the cavity walls (two side walls plus the bottom wall) is approximated by that on a flat plate with each cavity wall being treated as a single plate; the drag D_3 is equal to the sum of friction forces exerted on the cavity recirculating flow by the cavity walls. By use of the friction formulas for flow on a flat plate [12], the following equations are obtained for estimating D_3 . (The value of D_3 in a deep cavity with $H/B > 1$ is taken to be the same as that in a square cavity. Justifications will be described later.)

Labyrinth Seals with Rectangular Cavities (Fig. 2a)

For a laminar boundary layer on the cavity wall with $Re_\ell \leq 500,000$, we have

$$D_3 = 0.664\rho\nu^{0.5}WU_c^{1.5} (B^{0.5} + 2H^{0.5}) \quad \text{for } H/B < 1 \quad (8)$$

and

$$D_3 = 1.992\rho v^{0.5} W B^{0.5} U_c^{1.5} \quad \text{for } H/B \geq 1. \quad (9)$$

For a turbulent boundary layer on the cavity wall with $Re_\ell > 500,000$, we have

$$D_3 = 0.036\rho v^{0.2} W U_c^{1.8} (B^{0.8} + 2H^{0.8}) \quad \text{for } H/B < 1 \quad (10)$$

and

$$D_3 = 0.108\rho v^{0.2} W B^{0.8} U_c^{1.8} \quad \text{for } H/B \geq 1. \quad (11)$$

Similarly, for recirculating flow inside a thread (Fig. 2b) it is also assumed that the boundary-layer flow exists along two lateral walls of the thread at $Re_c \geq$ an order of 100 (based on the thread breadth).

Labyrinth Seals with Helical Threads (Fig. 2b)

For a laminar boundary layer on the thread wall with $Re_\ell \leq 500,000$, we have

$$D_3 = 1.328\rho v^{0.5} W A^{0.5} U_c^{1.5} \quad \text{for } A/B < 1 \quad (12)$$

and

$$D_3 = 1.328\rho v^{0.5} W B^{0.5} U_c^{1.5} \quad \text{for } A/B \geq 1. \quad (13)$$

For a turbulent boundary layer on the thread wall with $Re_\ell > 500,000$, we have

$$D_3 = 0.072\rho v^{0.2} W A^{0.8} U_c^{1.8} \quad \text{for } A/B < 1 \quad (14)$$

and

$$D_3 = 0.072\rho v^{0.2} W B^{0.8} U_c^{1.8} \quad \text{for } A/B \geq 1. \quad (15)$$

Equations (9) and (11) apply for both square and deep cavities with $H/B \geq 1$, and Eqs. (13) and (15) apply for the threads with $A/B \geq 1$. Justifications for doing this are described below. For recirculating flow

in a square or shallow cavity, there are generally a primary vortex in the core and two small corner vortices on the bottom wall (Fig. 5). (The latter are driven by the shear force from the former.) As the height of the cavity becomes larger than its breadth, experimental flow visualizations [17,18] and numerical solutions [17, 18, 25, 26] for $H/B = 2$ have shown that a second core vortex exists underneath the primary vortex, which is located right underneath the moving (top) wall. However, numerical solutions have shown that the recirculating speed of the second vortex is approximately two orders of magnitude smaller than that of the primary one. As the height of the cavity becomes larger than twice its breadth, there may be more than two vortices in the cavity. Numerical solutions of Pan and Acrivos [18] with $H/B = 5$ show that there are four vortices in the core — the primary vortex is on top, followed by the second, third, and fourth. The recirculating speed of the second vortex is also approximately two orders of magnitude smaller than that of the primary one and, in turn, the speed of the third one is about two orders of magnitude smaller than that of the second.

The important point is that in a finite cavity ($H/B \leq 5$), the primary vortex is predominant over the other vortices in the core and its height (defined as the vertical distance between the top cavity wall and the lower stagnation point of the vortex) is approximately equal to one cavity breadth. This is the reason that, for flow in a deep cavity ($H/B > 1$) with a finite depth ($H/B \leq 5$), the drag D_3 that acts on the main channel flow in the seal (Fig. 2) is taken to be the same as that in a square cavity [see Eqs. (9) and (11)].

However, this statement may no longer be valid for flow in an infinite cavity ($H/L \geq 10$); the experiment of Pan and Acrivos [18] for flow in a cavity with $H/B = 10$ (to simulate the infinite cavities) showed that the height of the primary vortex increases from a value of $1 B$ up to $1.7 B$ as Re_c increases from approximately 340 to 4000. (They also indicated that the height of the primary vortex is approximately proportional to $(Re_c)^{0.5}$ in the range of $1500 \leq Re_c \leq 4000$, the highest value in their experiment.)

For recirculating flow in a thread as shown in Fig. 2b, the author has found no flow visualization studies nor numerical solutions in the

literature. However, it is likely that the arguments for rectangular cavities can also be applied to the threads with various values of A/B.

The maximum boundary-layer velocity in the cavity is given by

$$U_c = C_4 U, \quad (16)$$

where C_4 is approximately in the range of 0.25 to 0.62 (Fig. 6).

Substituting Eqs. (3) through (7), Eqs. (8) through (11), and Eq. (16) into Eq. (2) yields the following equations for various flow conditions in straight labyrinth seals with rectangular cavities (Fig. 1a).

For laminar channel flow and laminar boundary-layer cavity flow with $Re \leq 2000$ and $Re_\ell \leq 500,000$, we have

$$\Delta P = 6C_2 \rho \nu C^{-2} (2S - B)U + 0.664 \rho \nu^{0.5} C^{-1} \times (B^{0.5} + 2H^{0.5})(C_4 U)^{1.5} \quad \text{for } H/B < 1 \quad (17)$$

and

$$\Delta P = 6C_2 \rho \nu C^{-2} (2S - B)U + 1.992 \rho \nu^{0.5} \times C^{-1} B^{0.5} (C_4 U)^{1.5} \quad \text{for } H/B \geq 1. \quad (18)$$

For laminar channel flow and turbulent boundary-layer cavity flow with $Re \leq 2000$ and $Re_\ell > 500,000$, we have

$$\Delta P = 6C_2 \rho \nu C^{-2} (2S - B)U + 0.036 \rho \nu^{0.2} C^{-1} \times (B^{0.8} + 2H^{0.8})(C_4 U)^{1.8} \quad \text{for } H/B < 1 \quad (19)$$

and

$$\Delta P = 6C_2 \rho \nu C^{-2} (2S - B)U + 0.108 \rho \nu^{0.2} \times C^{-1} B^{0.8} (C_4 U)^{1.8} \quad \text{for } H/B \geq 1. \quad (20)$$

For turbulent channel flow and laminar boundary-layer cavity flow with $Re > 2000$ and $Re_\ell \leq 500,000$, we have

$$\Delta P = 0.0333 C_3 \rho \nu^{0.25} C^{-1.25} (2S - B)U^{1.75} + 0.664 \rho \nu^{0.5} C^{-1} (B^{0.5} + 2H^{0.5})(C_4 U)^{1.5} \quad \text{for } H/B < 1 \quad (21)$$

and

$$\Delta P = 0.0333C_3\rho\nu^{0.25}C^{-1.25}(2S - B)U^{1.75} \\ + 1.992\rho\nu^{0.5}C^{-1}B^{0.5}(C_4U)^{1.5} \quad \text{for } H/B \geq 1 . \quad (22)$$

For turbulent channel flow and turbulent boundary-layer cavity flow with $Re > 2000$ and $Re_\ell > 500,000$, we have

$$\Delta P = 0.0333C_3\rho\nu^{0.25}C^{-1.25}(2S - B)U^{1.75} \\ + 0.036\rho\nu^{0.2}C^{-1}(B^{0.8} + 2H^{0.8})(C_4U)^{1.8} \quad \text{for } H/B < 1 \quad (23)$$

and

$$\Delta P = 0.0333C_3\rho\nu^{0.25}C^{-1.25}(2S - B)U^{1.75} \\ + 0.108\rho\nu^{0.2}C^{-1}B^{0.8}(C_4U)^{1.8} \quad \text{for } H/B \geq 1 . \quad (24)$$

Similarly, substituting Eqs. (3) through (7), Eqs. (12) through (15), and Eq. (16) into Eq. (2) yields the following equations for various flow conditions in straight labyrinth seals with threads (Fig. 1b).

For laminar channel flow and laminar boundary-layer thread flow with $Re \leq 2000$ and $Re_\ell \leq 500,000$, we have

$$\Delta P = 6C_2\rho\nu C^{-2}(2S - B)U + 1.328\rho\nu^{0.5}C^{-1}A^{0.5}(C_4U)^{1.5} \quad \text{for } A/B < 1 \quad (25)$$

and

$$\Delta P = 6C_2\rho\nu C^{-2}(2S - B)U + 1.328\rho\nu^{0.5}C^{-1}B^{0.5}(C_4U)^{1.5} \quad \text{for } A/B \geq 1 . \quad (26)$$

For laminar channel flow and turbulent boundary-layer thread flow with $Re \leq 2000$ and $Re_\ell > 500,000$, we have

$$\Delta P = 6C_2\rho\nu C^{-2}(2S - B)U + 0.072\rho\nu^{0.2}C^{-1}A^{0.8}(C_4U)^{1.8} \quad \text{for } A/B < 1 \quad (27)$$

and

$$\Delta P = 6C_2\rho\nu C^{-2}(2S - B)U + 0.072\rho\nu^{0.2}C^{-1}B^{0.8}(C_4U)^{1.8} \quad \text{for } A/B \geq 1 . \quad (28)$$

For turbulent channel flow and laminar boundary-layer thread flow with $Re > 2000$ and $Re_\ell \leq 500,000$, we have

$$\Delta P = 0.0333C_3\rho v^{0.25}C^{-1.25}(2S - B)U^{1.75} + 1.328\rho v^{0.5}C^{-1}A^{0.5}(C_4U)^{1.5} \quad \text{for } A/B < 1 \quad (29)$$

and

$$\Delta P = 0.0333C_3\rho v^{0.25}C^{-1.25}(2S - B)U^{1.75} + 1.328\rho v^{0.5}C^{-1}B^{0.5}(C_4U)^{1.5} \quad \text{for } A/B \geq 1 \quad (30)$$

For turbulent channel flow and turbulent boundary-layer thread flow with $Re > 2000$ and $Re_\ell > 500,000$, we have

$$\Delta P = 0.0333C_3\rho v^{0.25}C^{-1.25}(2S - B)U^{1.75} + 0.072\rho v^{0.2}C^{-1}A^{0.8}(C_4U)^{1.8} \quad \text{for } A/B < 1 \quad (31)$$

and

$$\Delta P = 0.0333C_3\rho v^{0.25}C^{-1.25}(2S - B)U^{1.75} + 0.072\rho v^{0.2}C^{-1}B^{0.8}(C_4U)^{1.8} \quad \text{for } A/B \geq 1 \quad (32)$$

Similarly, for laminar channel flow in a seal with no cavities or threads, we have

$$\Delta P = 12C_2\rho vC^{-2}SU \quad (33)$$

For turbulent channel flow in a seal with no cavities or threads, we have

$$\Delta P = 0.0666C_3\rho v^{0.25}C^{-1.25}SU^{1.75} \quad (34)$$

In order to calculate the mean channel velocity U from one of the equations given above [Eqs. (17) to (34)], the value of ΔP is calculated first from Eq. (1) and then substituted into the equation chosen to obtain U by trial and error, which is straightforward since ΔP monotonically increases with U . Then the channel and boundary-layer Reynolds numbers

(Re and Re_ℓ) are calculated (from U) to determine if the right equation has been used in obtaining the channel velocity. As a first approximation to the problem, it is recommended that the following values be used for the coefficients: $K_c = K_e = 0$, $C_2 = C_3 = 1$, and $C_4 = 0.4$. The value of U thus obtained will be "larger" than the value obtained if the entrance and exit losses of the seal as well as the hydrodynamic entry length of the seal have been taken into account. However, if the value of U is already tolerable, the calculation can be terminated. Otherwise, more realistic values for those coefficients should be used.

The values of K_c and K_e perhaps can be estimated from those given in Kays and London [10] (note that the maximum value of either K_c or K_e is approximately equal to unity), the value of C_2 or C_3 can be estimated from the velocity of the first approximation (obtained with $C_2 = C_3 = 1$) with the use of existing friction coefficients taking entry length into account as given in references [11,30], and the value of C_4 can be estimated from Fig. 6. Furthermore, since the turbulent channel flow will become fully developed with a much shorter entry length (than that of the laminar flow) and since the seal length L is generally much greater than the clearance C , $C_3 = 1$ is probably a good approximation. However, for laminar channel flow in the seal (with $Re \leq 2000$), the flow will not fully develop until a flow length of approximately $0.02 CRe$ has been reached [11, 30]; for the seal with L larger than this hydrodynamic entry length, $C_2 \approx 1 + 0.018 CRe/L$, which is estimated by the present author from Han's analytical result for flow in a channel [30].

The volumetric leakage through the seal is given by

$$Q = 2\pi RCU , \quad (35)$$

and the mass flow rate leaking through the seal is

$$M = \rho Q = 2\pi\rho RCU . \quad (36)$$

RESULTS AND DISCUSSION

Straight labyrinth seals have been used to minimize the flow leakage in the test sections of two 19-pin sodium-cooled bundles, designated as

THORS bundle 3C [8] and bundle 6A [9], to simulate the fuel assemblies of the liquid metal fast breeder reactor (LMFBR). The seals are formed in an annular passage with helical threads at the outer wall as shown in Fig. 1b and have the following dimensions: $S = 3.05$ mm, $B = 0.6375$ mm, $A = 1.23$ mm, $L = 25.4$ mm, $N = 8.33$, $R = 48.9$ mm, and $C = 0.0229$ and 0.0343 mm for bundles 3C and 6A, respectively [8, 9]. Fluid properties used in the calculations are for liquid sodium at the experimental temperature of 443°C ($\rho = 845$ kg/m³ and $\nu = 3.05 \times 10^{-7}$ m²/s) and at 382°C ($\rho = 860$ kg/s and $\nu = 3.35 \times 10^{-7}$ m²/s) for bundles 3C and 6A, respectively. Equations (1) and (26) are used with $C_1 = C_2 = 1$, $K_c = K_e = 0$, and $C_4 = 0.4$.

Table 1 presents the volumetric sodium leakage Q through the labyrinth seal in THORS bundle 3C at various total driving pressure drops across the seal [ΔP defined in Eq. (1)]; the seal leakage is estimated to be less than 1% of the total flow in the test section. Table 2 presents the volumetric sodium leakage through the labyrinth seal in THORS bundle 6A, which has a seal clearance (C) 50% larger than that in bundle 3C; the seal leakage is estimated to be less than 2% of the total flow in the test section. Since the seal leakage is no more than 2% of the total test-section flow, it is deemed to be negligible.

The corresponding mass leak rates of sodium (M) passing through the labyrinth seals in THORS bundles 3C and 6A are shown in Fig. 7. Obviously,

Table 1. Volumetric leakages of sodium through the labyrinth seal in THORS bundle 3C (sodium properties at 443°C are used in calculations)

Total test-section flow [ℓ/s (gpm)]	Total driving pressure drop ΔP [kPa (psi)]	Seal leakage Q [ℓ/s (gpm)]	Percentage of total flow (%)
0.498 (7.9)	6.895 (1.0)	0.000360 (0.0057)	0.07
0.908 (14.4)	20.7 (3.0)	0.00108 (0.0171)	0.12
1.29 (20.4)	49.6 (7.2)	0.00258 (0.0409)	0.20
2.73 (43.2)	221 (32)	0.0114 (0.181)	0.42
3.71 (58.8)	379 (55)	0.0196 (0.310)	0.53
4.54 (72.0)	703 (102)	0.0362 (0.573)	0.79

Table 2. Volumetric leakages of sodium through the labyrinth seal in THORS bundle 6A (sodium properties at 382°C are used in calculations)

Total test-section flow [ℓ/s (gpm)]	Total driving pressure drop ΔP [kPa (psi)]	Seal leakage Q [ℓ/s (gpm)]	Percentage of total flow (%)
0.132 (2.1)	4.00 (0.58)	0.000630 (0.00998)	0.48
0.252 (4.0)	7.58 (1.1)	0.00119 (0.0189)	0.47
0.524 (8.3)	19.3 (2.8)	0.00303 (0.0480)	0.58
0.770 (12.2)	35.2 (5.1)	0.00551 (0.0874)	0.71
1.05 (16.7)	57.9 (8.4)	0.00909 (0.144)	0.86
1.57 (24.9)	110 (15.9)	0.0171 (0.271)	1.1
2.07 (32.8)	174 (25.2)	0.0270 (0.428)	1.3
2.58 (40.9)	252 (36.5)	0.0389 (0.617)	1.5

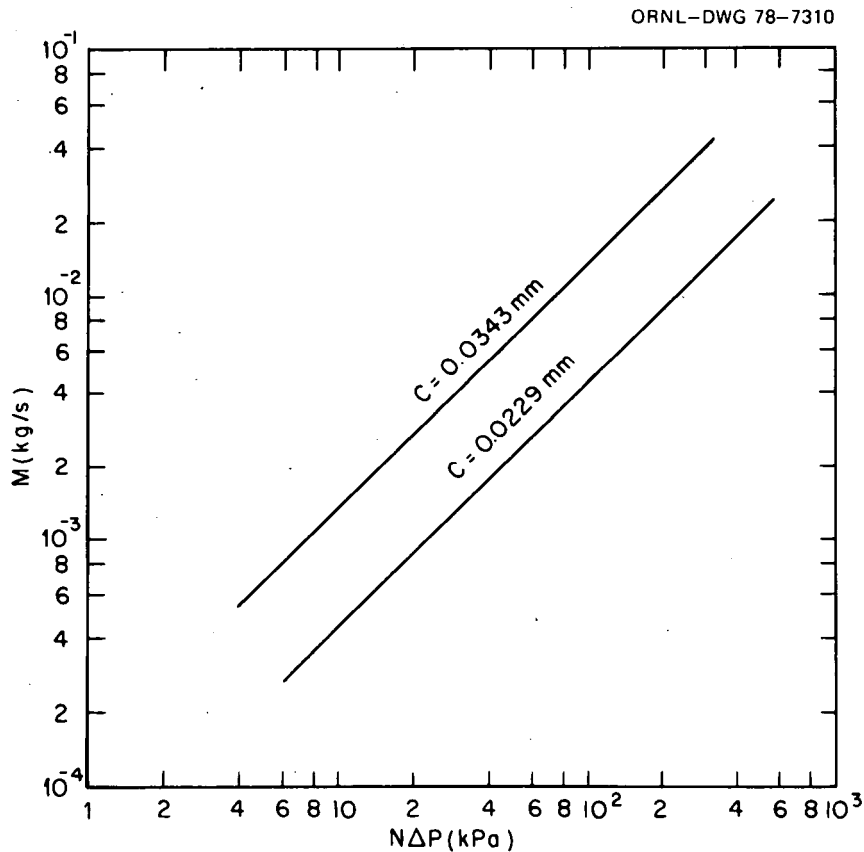


Fig. 7. Mass leak rate as a function of total driving pressure drop and seal clearance for a straight labyrinth seal with helical threads.

the mass leak rate increases with the driving pressure drop and seal clearance. As the seal clearance is increased by 50% from 0.0229 to 0.0343 mm, the mass leak rate is increased by approximately 200%. (It should be noted that slightly different properties have been used in calculating the curves in Fig. 7. Nevertheless, the effect on the change of seal leakage is insignificant.) From the energy balance using the flow and temperature measurements in the pin bundles, it was estimated that the leak rate through the seal was less than 10% of the total flow through the experimental assembly; the analytical results shown in Fig. 7 and Tables 1 and 2 are indeed within this range.

To further evaluate the validity of this model, comparisons were also made with some existing gas data. Zabriskie and Sternlicht [4] correlated the mass flow rate as a function of P_{out}/P_{in} for gas leakages measured in a cavity-type labyrinth seal at two seal clearances (Fig. 5 of their paper). (Dimensions of the seal are $S = 8.48$ mm, $B = 8.23$ mm, $H = 9.53$ mm, $N = 29$, and $C = 0.584$ and 1.37 mm.) Since the present model is applicable to incompressible fluids only, the data chosen for comparison are limited to those for which the value of P_{out}/P_{in} is close to 1 and the resulting Mach number (Ma) is still small [31, 10]. Table 3 presents the comparisons between the experimental results [4] and theoretical calculations, in which Eqs. (1) and (22) were used with $C_1 = K_c = K_e = 0$, $C_3 = 1$, and $C_4 = 0.4$ with air properties evaluated at average seal pressure [$= 0.5 (P_{in} + P_{out})$] and an arbitrarily chosen temperature of 21°C . Theoretical calculations are of the same order of magnitude as the experimental results for gas, although the former are approximately 140 to 290% higher than the latter. In calculations, the entrance and exit losses of the seal as well as the hydrodynamic entry-length effect of the seal have been neglected; otherwise, the resulting channel velocity in the seal U should be somewhat smaller and the comparisons would be better. Nevertheless, the simple model predicts the correct order of magnitude of fluid leakage through the labyrinth seal despite the complex seal geometry involved.

A topic of interest to a seal designer is the comparison of flow leakage among labyrinth seals with cavities (Fig. 1a), with threads (Fig. 1b), and without cavities or threads. According to the model, the cavity-

Table 3. Comparisons between experimental results [4] and theoretical calculations for air passing through a labyrinth seal

	Case No.				
	1	2	3	4	5
C (mm)	0.584	0.584	0.584	1.37	1.37
P_{out}/P_{in}	0.83	0.80	0.71	0.83	0.80
P_{in}^* [kPa (psia)]	138 (20.0)	112 (16.3)	148 (21.4)	138 (20.0)	112 (16.3)
U_{exp} (m/s)	31	34	43	35	42
U_{cal} (m/s)	75	80	107	136	145
U_{cal}/U_{exp}	2.4	2.4	2.5	3.9	3.5
$(U_{cal} - U_{exp})/U_{exp}$ (%)	140	140	150	290	250
$Ma = U_{exp}/a$	0.090	0.099	0.12	0.10	0.12

* Arbitrarily chosen values.

type seal offers more flow resistance than the thread type (due to three walls in a cavity vs two walls in a thread), if all other conditions are kept the same (e.g., C, B, L, S, fluid properties, and seal pressure drop). A comparison of Eq. (18) with Eq. (26) shows that the second term on the right-hand side of the former is 50% larger than that of the latter. The same conclusion can also be reached by comparing Eqs. (20) and (28), Eqs. (22) and (30), or Eqs. (24) and (32). Consequently, the flow leakage through the labyrinth seal with cavities is likely to be smaller than that through the seal with threads.

The comparison of flow leakage for a seal with cavities and that with no cavities depends on several parameters, including seal clearance C, cavity breadth B, cavity height H, fluid properties, and pressure drop through the seal. For most designs, fluid properties and seal pressure drop are given; by choosing various values for seal clearance and cavity dimensions (generally under the constraint of the cost and operating conditions of the system where the seal is in use), the seal leakage can be estimated from one of Eqs. (17) through (24). The result can be compared with the flow leakage through a seal with no cavities, which can be easily calculated from either Eq. (33) or Eq. (34). One can then decide

which type of seal to use in his system. Similarly, a comparison can also be made between the seal with threads and that with no threads.

CONCLUSIONS

An analytical model for estimating the leakage of incompressible fluids through straight labyrinth seals has been described. Recent developments in theoretical and experimental studies of recirculating flow inside rectangular cavities and of flow in a channel have been incorporated in the model to solve a practical problem. The approach used in this model is different from those of previous ones for compressible fluids in which the gas-dynamics laws with some empirical coefficients determined from gas data were used. The seal leakages predicted by the model are in reasonable agreement with those measured indirectly in sodium and those obtained for gas at low Mach number and small pressure variations.

It can be concluded from this study that the labyrinth seal formed with cavities (Fig. 1a) has less leakage than the one formed with threads (Fig. 1b) if all other conditions are the same. Furthermore, the fluid leakage through straight labyrinth seals (for both cavity and thread types) is strongly dependent upon the seal clearance and pressure drop: $M \propto C^a (\Delta P)^b$, where $1.5 < a < 3$ and $0.5 < b < 1$.

NOMENCLATURE

A	Lateral dimension of seal thread (Fig. 1)
a	Speed of sound
B	Breadth of seal cavity or thread (Fig. 1)
C	Radial clearance of seal
C_1	Elevation coefficient ($ C_1 \leq 1$)
C_2	Laminar entry-length coefficient (to account for the larger pressure drop in the hydrodynamic entry length above that in the fully developed region, $C_2 \geq 1$)
C_3	Turbulent entry-length coefficient ($C_3 \geq 1$)
C_4	Ratio of U_c/U ($C_4 < 1$)
D	Drag force (Fig. 2)

g	Acceleration of gravity
H	Height of seal cavity (Fig. 1)
K_c	Abrupt contraction (entrance) coefficient at seal inlet
K_e	Abrupt expansion (exit) coefficient at seal outlet
L	Seal length in flow direction (Fig. 1)
M	Mass leak rate [Eq. (36)]
Ma	Mach number, $Ma = U/a$
N	Total number of throttlings in seal, $N = L/S$
P	Pressure
ΔP	Average driving pressure drop of each throttling [Eq. (1)]
Q	Volumetric leak rate [Eq. (35)]
R	Radius of the annular seal passage or the channel (Fig. 1)
Re	Reynolds number based on the hydraulic diameter of seal channel, $Re = U2C/\nu$
Re_c	Cavity (or thread) Reynolds number, $Re_c = UB/\nu$
Re_ℓ	Reynolds number for boundary-layer flow inside the cavity, $Re_\ell = U_c B/\nu = C_4 Re_c$ (except for $A/B < 1$, $Re_\ell = U_c A/\nu$)
S	Axial length of a seal throttling (Fig. 1)
u	Local velocity inside the seal cavity (parallel to the wall)
U	Mean velocity in the annular seal passage (namely, the channel)
U_c	Maximum boundary-layer velocity inside seal cavity or thread, $U_c = C_4 U$
W	Seal depth (normal to the plot in Fig. 1), $W = 2\pi R$
y	Coordinate normal to the cavity wall

Subscripts

cal	Value calculated from the model
exp	Experimentally determined value
in	Seal inlet
out	Seal outlet

Greek

δ	Boundary layer thickness (based on U_c)
ν	Average kinematic viscosity of fluid
ρ	Average fluid density
τ_0	Wall shear stress

REFERENCES

1. A. Egli, "The Leakage of Steam through Labyrinth Seals," *ASME Trans.* 57, 115-22 (April 1935).
2. H. A. Rothbart, *Mechanical Design and Systems Handbook*, pp. 24-34 to 24-38, McGraw-Hill, New York, 1964.
3. F. E. Heffner, "A General Method for Correlating Labyrinth-Seal Leak-Rate Data," *J. Basic Eng.* 265-75 (June 1960).
4. W. Zabriskie and B. Sternlicht, "Labyrinth-Seal Leakage Analysis," *J. Basic Eng.* 81, 332-40 (September 1959).
5. W. J. Kearton, "The Flow of Air through Radial Labyrinth Glands," *Proceedings of the Institution of Mechanical Engineers*, Vol. 169, 1955.
6. J. Jerie, "Flow through Straight-through Labyrinth Seals," *Proceedings of the Seventh International Congress for Applied Mechanics*, Vol. 2, pp. 70-82, 1948.
7. T. Baumeister, *Standard Handbook for Mechanical Engineers*, 7th ed., pp. 8-192, 9-68-9-69, McGraw-Hill, New York, 1967.
8. M. H. Fontana and J. L. Wantland, *Breeder Reactor Safety and Core Systems Programs Progress Report for April-June 1977*, ORNL/TM-6020, pp. 5-15 (1977).
9. J. L. Wantland et al., *Steady-State Sodium Tests in a 19-Pin Full-Length Simulated LMFBR Fuel Assembly - Record of Steady-State Experimental Data for THORS Bundle 6A*, ORNL/TM-6106 (March 1978).
10. W. M. Kays and A. L. London, *Compact Heat Exchangers*, 2d ed., pp. 92-97, McGraw-Hill, New York, 1967.
11. W. M. Kays, *Convective Heat and Mass Transfer*, pp. 53-63, McGraw-Hill, New York, 1966.
12. H. Schlichting, *Boundary-Layer Theory*, 6th ed., pp. 117-33 and 560-605 and 19, McGraw-Hill, New York, 1968.
13. G. K. Batchelor, "On Steady Laminar Flow with Closed Streamlines at Large Reynolds Number," *J. Fluid Mech.* 1, 177-90 (1956).
14. H. B. Squire, "Note on the Motion inside a Region of Recirculation (Cavity Flow)," *J. Roy. Aeronaut. Soc.* 60, 203-8 (1956).
15. P. K. Chang, *Separation of Flow*, pp. 276-83, Pergamon Press, New York, 1973.

16. A. Roshko, *Some Measurements of Flow in a Rectangular Cutout*, NACA-TN-3488 (1955).
17. R. D. Mills, "Numerical Solutions of the Viscous Flow Equations for a Class of Closed Flows," *J. Roy. Aeronaut. Soc.* 69, 714-18 (1965).
18. F. Pan and A. Acrivos, "Steady Flows in Rectangular Cavities," *J. Fluid Mech.* 28, 643-55 (1967).
19. D. J. Maull and L. F. East, "Three-Dimensional Flow in Cavities," *J. Fluid Mech.* 16, 620-32 (1963).
20. H. W. Townes and R. H. Sabersky, "Experiments on the Flow over a Rough Surface," *Int. J. Heat Mass Transfer* 9, 729-38 (1966).
21. T. C. Reiman and R. H. Sabersky, "Laminar Flow over Rectangular Cavities," *Int. J. Heat Mass Transfer* 11, 1083-85 (1968).
22. O. R. Burggraf, "Analytical and Numerical Studies of the Structure of Steady Separated Flows," *J. Fluid Mech.* 24, 113-51 (1966).
23. M. Nallasamy and K. Krishna Prasad, "On Cavity Flow at High Reynolds Numbers," *J. Fluid Mech.* 79, 391-414 (1977).
24. A. D. Gosman et al., *Heat and Mass Transfer in Recirculating Flows*, pp. 162-65, Academic Press, New York, 1969.
25. J. D. Bozeman and C. Dalton, "Numerical Study of Viscous Flow in a Cavity," *J. Comput. Phys.* 12, 348-63 (1973).
26. D. Greenspan, "Numerical Studies on Prototype Cavity Flow Problems," *Comput. J.* 12, 88-93 (1969).
27. V. O'Brien, "Closed Streamlines Associated with Channel Flow over a Cavity," *Phys. Fluids* 15, 2089-97 (1972).
28. B. S. Jagadish, "Numerical Study of Transient and Steady Induced Symmetric Flows in Rectangular Cavities," ASME Paper No. 77-FE-17 (June 1977).
29. L. N. Tao and W. F. Donovan, "Through-Flow in Concentric and Eccentric Annuli of Fine Clearance with and without Relative Motion of the Boundaries," *Trans. ASME* 77(8), 1291-99 (November 1955).
30. L. S. Han, "Hydrodynamic Entrance Lengths for Incompressible Flow in Rectangular Ducts," *J. Appl. Mech.* 27, 403-9 (1960).
31. H. W. Liepmann and A. Roshko, *Elements of Gasdynamics*, pp. 50-53, Wiley, New York, 1957.

ORNL/TM-6373
 Dist. Category UC-79,
 -79e, -79p

Internal Distribution

- | | |
|----------------------|--------------------------------------|
| 1. A. H. Anderson | 36. B. H. Montgomery |
| 2. R. S. Booth | 37. R. L. Moore |
| 3. N. E. Clapp | 38. R. H. Morris |
| 4. C. W. Collins | 39. F. R. Mynatt |
| 5. W. B. Cottrell | 40. L. C. Oakes |
| 6. J. F. Dearing | 41. L. F. Parsly |
| 7. G. F. Flanagan | 42. P. Patriarca |
| 8. M. H. Fontana | 43. R. J. Ribando |
| 9. D. N. Fry | 44. J. P. Sanders |
| 10. P. W. Garrison | 45. Myrtlelen Sheldon |
| 11. P. A. Gnadt | 46. W. H. Sides |
| 12. G. W. Greene | 47. M. J. Skinner |
| 13. A. G. Grindell | 48. C. M. Smith |
| 14. P. M. Haas | 49. I. Spiewak |
| 15-24. J. T. Han | 50. D. G. Thomas |
| 25. N. Hanus | 51. R. H. Thornton |
| 26. W. O. Harms | 52. E. T. Tomlinson |
| 27. R. A. Hedrick | 53. H. E. Trammell |
| 28. H. W. Hoffman | 54. D. B. Trauger |
| 29. P. R. Kasten | 55. J. L. Wantland |
| 30. T. S. Kress | 56. G. D. Whitman |
| 31. W. H. Leavell | 57-58. Central Research Library |
| 32. Milton Levenson | 59. Y-12 Document Reference Section |
| 33. R. E. MacPherson | 60-62. Laboratory Records Department |
| 34. C. D. Martin | 63. Laboratory Records (RC) |
| 35. R. W. McCulloch | |

External Distribution

64. Assistant Administrator for Nuclear Energy, DOE, Washington, D.C. 20545
- 65-66. Director, Division of Reactor Research and Technology, DOE, Washington, D.C. 20545
67. Director, Reactor Division, DOE, ORO
68. Research and Technical Support Division, DOE, ORO
- 69-308. For distribution as shown in TID-4500 under categories UC-79, -79e, -79p